Radiation-induced structural changes in chalcogenide glasses as revealed from Raman spectroscopy measurements

T.S. Kavetskyy
Ivan Franko Drohobych State Pedagogical University, Solid-State Microelectronics Laboratory,
24, I. Franko str., 82100 Drohobych, Ukraine

Abstract. Radiation-induced structural changes in the chalcogenide glasses of $(As_2S_3)_x(GeS_2)_{1-x}$ system with $x = 0.1$, 0.2, 0.4, and 0.6 corresponding to the chemical compositions $Ge_{28.125}As_{6.25}S_{65.625}$, $Ge_{23.5}As_{11.8}S_{64.7}$, $Ge_{15.8}As_{21}S_{63.2}$, and $Ge_{9.5}As_{28.6}S_{61.9}$, respectively, were studied using the Raman spectroscopy technique in detail. The polarized (VV) and depolarized (VH) Raman spectra were recorded separately for two identical samples in the unirradiated and γ-irradiated states which allowed performing all measurements under the same experimental conditions. The Raman spectra were considered in the regions of high-frequency excitations related with the molecular peak, and low-frequency excitations related with the boson peak. The depolarization ratio spectra for the unirradiated and γ-irradiated samples were examined, too. The differential Raman spectra in the high-frequency region between unirradiated and γ-irradiated samples were obtained only in the VH configuration, since no spectral variations in the VV configuration were detected for all the compositions studied. Employing the differential representation ($I_{\text{irrad.}}^{R} - I_{\text{unirrad.}}^{R}$) of the VH Raman spectra measured for the γ-irradiated ($I_{\text{irrad.}}^{R}$) and unirradiated ($I_{\text{unirrad.}}^{R}$) samples, it has been found out that the radiation-induced structural changes are significant only for the glass composition with $x = 0.4$, while these changes are practically absent in the case of the glass compositions with $x = 0.1$, 0.2, and 0.6. The applied differential procedure allows also to detect the radiation-induced effects in clusters of corner-shared and edge-shared tetrahedral, which was not possible with IR Fast Fourier Transform spectroscopy due to different activity of IR and Raman bands. In addition, it was shown that the controversial companion A_1^c mode at 370 cm^{-1} to the main 340 cm^{-1} A_1 symmetric mode of vibrations in corner-shared tetrahedra seems to be related mainly to the vibrations of edge-shared tetrahedra. The possible nanoscale structural mechanism to account for these spectral changes has been discussed.

Keywords: Raman spectroscopy, chalcogenide glasses, radiation modification.

1. Introduction

Chalcogenide glasses are known to be sensitive to external influences such as photoexposure [1-5] and high-energy ionizing irradiation (γ-quanta [6-10], accelerated electrons [10-13], protons [14]). A great number of results testify in favour of a phenomenological similarity between photo- and radiation-induced effects in these glasses despite the role of chemical composition, preparation method and thermal pre-history of samples.

The Raman scattering technique is a powerful experimental tool for investigation of vibrational properties and structure of materials, and, in particular, chalcogenide glasses. In the early 80-s, this method was successfully applied to study reversible photostructural

transformations in amorphous As_2S_3 [1, 2, 15-17]. It was shown with account of the obtained Raman spectra that this effect is accompanied by switching of heteropolar (or heteronuclear) bonds into homopolar (or homonuclear) ones [15, 16]. This method also allowed explaining the optically induced crystal-to-amorphous-state transition in As_2S_3 as non-thermal effect probably promoted by a high density of induced defects [17]. Besides, Raman scattering measurements along with EXAFS data clearly indicated a reversible increase in the coordination number of Se in the photoexcited state due to additional dynamic bonds between pairs of over-coordinated sites [18]. Application of Raman spectroscopy is also reasonable for better understanding the photostructural changes in ternary chalcogenide glassy systems [3-5, 19, 20]. New evidence of light-induced structural changes in As–S glasses was obtained by photon energy dependent Raman spectroscopy [21].

In this work, Raman spectroscopy is used to study high-energy γ-irradiation-induced structural changes in chalcogenide glasses. The earlier obtained Raman results for the selected chalcogenide glass of $(As_2S_3)_x(GeS_2)_{1-x}$ system with $x = 0.4$ and chemical composition $Ge_{15.8}As_{21}S_{63.2}$ [22] showed that the radiation-induced shift of the main molecular band from 340 to 335 cm^{-1} takes place in the depolarized (VH) configuration. This shift was assigned due to structural transformations in the glass network under radiation. The aim of this work is to analyze deeper the radiation-induced structural changes in the $Ge_{15.8}As_{21}S_{63.2}$ glass and as compared to other alloys of the $(As_2S_3)_x(GeS_2)_{1-x}$ system with $x = 0.1$, 0.2, and 0.6 and corresponding chemical compositions $Ge_{28.125}As_{6.25}S_{65.625}$, $Ge_{23.5}As_{11.8}S_{64.7}$, and $Ge_{9.5}As_{28.6}S_{61.9}$, respectively. The Raman spectra will be considered in the regions of high-frequency excitations related with the molecular peak, and low-frequency excitations related with the boson peak. The depolarization ratio for the unirradiated and γ-irradiated samples will be examined, too. The radiation-induced structural changes will be detected in the differential representation ($I_{irrad.}^R - I_{unirrad.}^R$) of the VH Raman spectra measured for the γ-irradiated ($I_{irrad.}^R$) and unirradiated ($I_{unirrad.}^R$) samples.

2. Experimental

The investigated bulk glasses were prepared using the standard melt-quenching procedure with cooling in water as was described in detail elsewhere [23]. After synthesis the ingots were cut to the parallel disks (~1 mm in thickness), which then were polished to high optical quality. The disk glassy samples were tested separately in two structural configurations such as unirradiated (or reference) and γ-irradiated ones. Before experimental measurements the samples were annealed at 20-30 K below the glass transition temperature T_g during 1 hour [24].

The radiation treatment of the samples was performed by γ-quanta with the absorbed dose $\Phi = 2.41$ MGy and the average energy $E = 1.25$ MeV under the normal conditions of stationary radiation field created in the closed cylindrical cavity owing to concentrically maintained ^{60}Co sources. No special measurements were done to prevent the uncontrolled thermal annealing of the sample, but the maximum temperature in irradiating camera did not exceed 330 K during the whole period of γ-treatment (about 2 to 3 months).

The Raman spectra were excited using 647.1 nm Kr^+ laser line at a power density of 40 mW in a pseudo-backscattering geometry. Collected scattered light was analyzed by SPEX 1403 double monochromator operated at a spectral bandpass of 1.5 cm^{-1} and detected by a cooled photomultiplier. The Raman spectra were recorded separately in both VV and VH configurations corresponding to parallel (VV "vertical-vertical") and crossed (VH "vertical-horizontal") polarizations between incident and scattered light. In order to make the comparative analysis of the data obtained for the unirradiated and γ-irradiated samples, the measured Raman spectra were normalized to the intensity of the main molecular band at 340 cm^{-1}. All the measurements were made at room temperature.

3. Results

The normalized Raman spectra of unirradiated and γ-irradiated samples with $x = 0.4$ (chemical composition $Ge_{15.8}As_{21}S_{63.2}$) in the VV and VH configurations are shown in Fig. 1 [22, 25]. One can see that no change in the Raman spectra for the VV configuration is observed, while the spectrum for the VH configuration is sufficiently modified in the γ-irradiated state. As a result of radiation-induced effect on the glass structure, the shift of the main molecular band at 342 cm^{-1} to the new position at 335 cm^{-1} is detected. Besides, the radiation-induced changes in the intensity of the bands at 490, 430, 370, 237, and 205 cm^{-1} are also identified.

The depolarization ratio spectra ($\rho(\omega) = I_{VH}/I_{VV}$), the ratio of the scattering intensity in two configurations (VH/VV) within the whole spectral range for the unirradiated and γ-irradiated samples with $x = 0.4$ are presented in Fig. 2. The observed two local minima in the range $200 – 250$ cm^{-1} and one local minimum in the range $300 – 400$ cm^{-1} and at 430 cm^{-1} for the unirradiated sample could be influenced by the depolarization ratio of the optical TO-type phonon vibrational bands. In the case of γ-irradiated sample, the sharper drop in the depolarization ratio at $200 – 250$ cm^{-1}, $300 – 400$ cm^{-1} and 430 cm^{-1} is detected with twining (two local minima) within the range of 300 to 400 cm^{-1}. The plateau between 100 and 200 cm^{-1} as well as rise to higher values ($\rho(\omega) \sim 0.6$) along with Raman frequency shift decreasing below 100 cm^{-1} (the low-frequency Raman spectra region or region of the so-called "boson

peak") is also observed as more clearly pronounced in the γ-irradiated state (see insert in Fig. 2).

Fig. 3 illustrates the differential normalized VH Raman spectrum ($I^R_{\text{irrad.}} - I^R_{\text{unirrad.}}$) between γ-irradiated ($I^R_{\text{irrad.}}$) and unirradiated ($I^R_{\text{unirrad.}}$) samples with $x = 0.4$ ($Ge_{15.8}As_{21}S_{63.2}$) as compared to the differential spectra of other alloys in the $(As_2S_3)_x(GeS_2)_{1-x}$ system with $x = 0.1$ ($Ge_{28.125}As_{6.25}S_{65.625}$), $x = 0.2$ ($Ge_{23.5}As_{11.8}S_{64.7}$), and $x = 0.6$ ($Ge_{9.5}As_{28.6}S_{61.9}$) [26]. One can see appearance of positive and negative intensity peaks only for the glass composition with $x = 0.4$, corresponding to the created and destructed covalent bonds, respectively, like to conventional IR FFT spectrum of additional γ-induced reflectivity [27], while the spectral changes are practically absent in the case of the glass compositions with $x = 0.1, 0.2$, and 0.6.
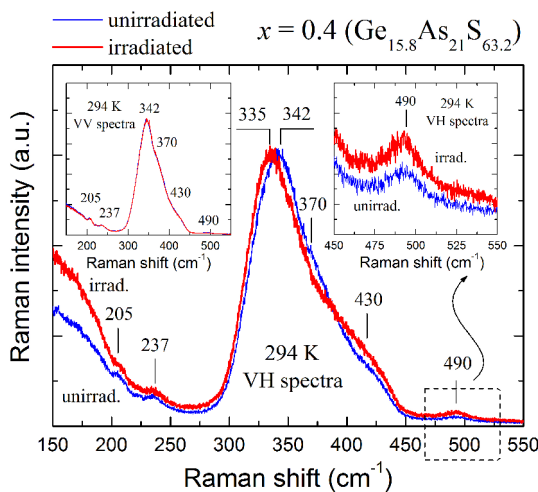

Fig. 1. The normalized VH Raman spectra for unirradiated and γ-irradiated glasses of the $(As_2S_3)_x(GeS_2)_{1-x}$ system with $x = 0.4$ ($Ge_{15.8}As_{21}S_{63.2}$). Inserts show corresponding Raman spectra in VV polarization (left) and VH polarization in the vicinity of 490 cm^{-1} band (right).
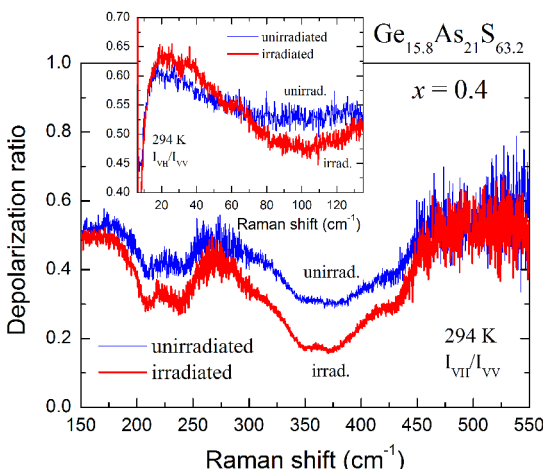

Fig. 2. The high-frequency depolarization ratio spectra ($\rho(\omega) = I_{VH}/I_{VV}$) for unirradiated and γ-irradiated glasses of the $(As_2S_3)_x(GeS_2)_{1-x}$ system with $x = 0.4$ ($Ge_{15.8}As_{21}S_{63.2}$). Insert shows respective low-frequency depolarization ratio spectra.

It must be noted that the radiation-induced changes in the VV and VH Raman spectra obtained are similar to the light-induced ones examined by Kolobov *et al.* [18] for amorphous a-Se film. As well as in the case of γ-irradiated and unirradiated $Ge_{15.8}As_{21}S_{63.2}$ glasses (Fig. 1), no significant changes in the Raman spectra between unilluminated and illuminated a-Se for the VV configuration and in the strongly modified Raman spectrum for the VH configuration with appearance of new bands in the photoexcited state of a-Se have been detected [18].

Fig. 4 shows the polarized-VV and depolarized-VH Raman spectra of $(As_2S_3)_{0.2}(GeS_2)_{0.8}$ glass taken as an example. The low-frequency vibrational region of the Raman spectrum in both VV and VH configurations is characterized by the presence of the excess quasi-elastic light scattering well fitted using the Theodorakopoulos-Jäckle model [28] as shown schematically by lines with arrows in insert of Fig. 4. The larger excess quasi-elastic light scattering is found for the VV configuration than for the VH one, and, thus, the low-frequency vibrational excitations called 'boson peaks' (BP) are analyzed using the Raman spectra recorded in the VH configuration.

Fig. 5 demonstrates the ratio of the BP intensity to that of the main molecular peak at 340 cm^{-1}, I_{bos}/I_{mol}, often attributed to the degree of disorder in amorphous solids on the medium-range order (MRO) scale [29-31] for the unirradiated and γ-irradiated $(As_2S_3)_x(GeS_2)_{1-x}$ glasses as a function of composition x. Insert of Fig. 5 displays the difference in the I_{bos}/I_{mol} values between γ-irradiated and unirradiated samples. The largest radiation-induced changes of the disorder degree are observed for the alloy with $x = 0.4$ ($Ge_{15.8}As_{21}S_{63.2}$), which agrees well with the detected radiation-induced shift of the main molecular band at 342 cm^{-1} to the new position at 335 cm^{-1} only for this compound (Fig. 1). In contrast to the BP intenisty, the BP position does not show changes under radiation, within experimental errors.

4. Discussion

Taking into account the VV and VH Raman spectra measured for the investigated sample with $x = 0.4$ in the unirradiated state, one can see the series of Raman bands at 490, 430, 370, 342, 237 and 205 cm^{-1} (Fig. 1). The same Raman bands are also observed for the unirradiated samples with $x = 0.1, 0.2$, and 0.6 (exception is the band at 370 cm^{-1}, which is not detected for the alloy with $x = 0.6$). The main band at 342 cm^{-1} is related to symmetric A_1-type bond stretching mode of GeS_4 tetrahedra and AsS_3 pyramids [30-34] with the former units being more likely as a glass and corresponds to the $(As_2S_3)_{0.4}(GeS_2)_{0.6}$ formula. The band at 370 cm^{-1} is attributed to the so-called A_1^c companion mode [34]. The band at 430 cm^{-1} is assigned to edge-shared tetrahedra [34, 35] or S−S dimers [34, 36] at the edge of the so-called "outrigger raft" clusters proposed for
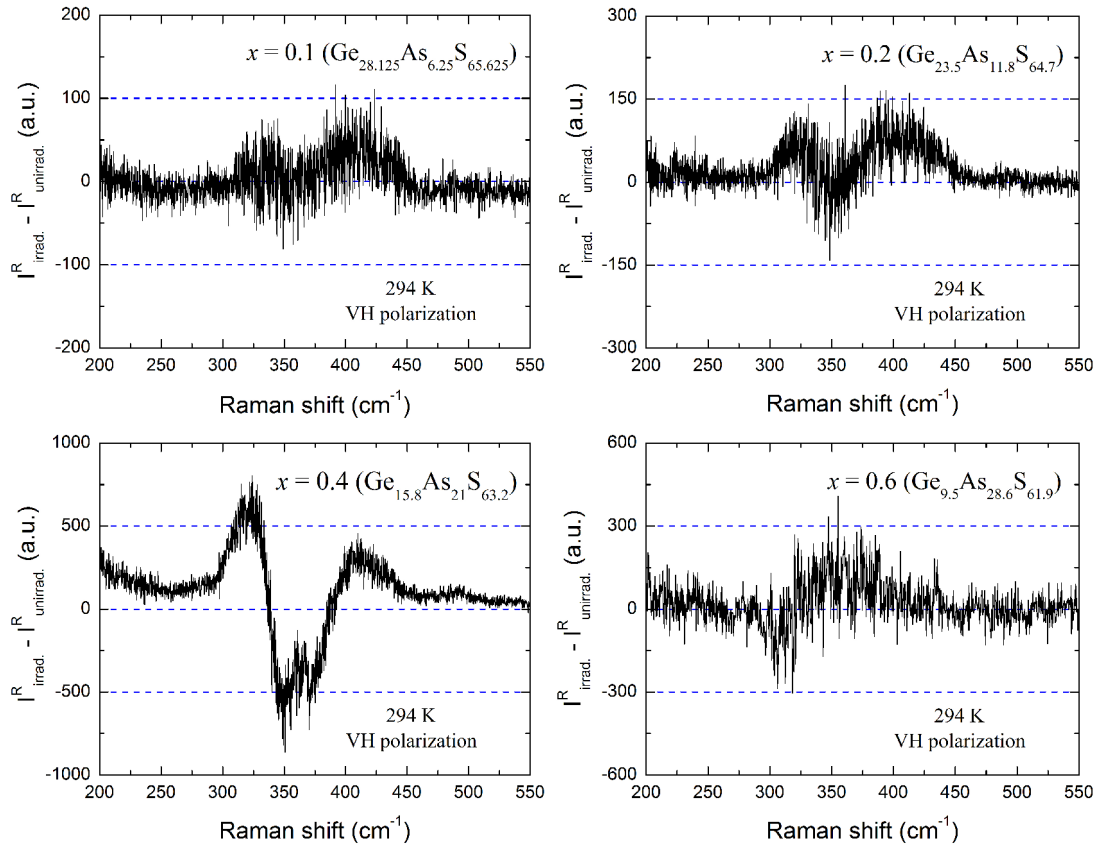
Fig. 3. The differential depolarized Raman spectra between γ-irradiated ($I_{irrad.}^{R}$) and unirradiated ($I_{unirrad.}^{R}$) glasses of $(As_2S_3)_x(GeS_2)_{1-x}$ ($x = 0.1, 0.2, 0.4, 0.6$) system. All the spectra were normalized to the intensity of the main Raman band at 340 cm^{-1} before substraction.

glassy g-GeSe(S)$_2$ [37]. The mode at 490 cm^{-1} corresponds to $S-S$ vibrations possibly in S_8 rings [38-42] or rather in covalent S_2 groups ($S-S$ disulfide bonds) [34, 43]. The very weak mode at 205 cm^{-1} is in accordance with the *ab-initio* calculated Raman peak at 211 and 212 cm^{-1} for $SGe_3 - S_{6/3}$ cluster in g-GeS$_2$ [44]. The mode at 237 cm^{-1} can be attributed to the structural units all having tri-coordinated S or Ge ($SGe_{3/3}$, $SGe_3 - S_{6/3}$, and $GeS_{3/3}$), as no other clusters have any peaks below 250 cm^{-1} in g-GeS$_2$ [44] as well as to vibrations of $As-As$ bonds in molecular fragments of As_4S_4 [41, 42]. Besides these Raman bands identified, appearance of the new band at 335 cm^{-1} instead of 342 cm^{-1} mode in the γ-irradiated state only for the sample with $x = 0.4$ testifies in favour of specific radiation-induced structural transformations in the glass matrix. This new band is detected in the VH configuration, and it should be attributed to the symmetric bond stretching mode of AsS$_3$ pyramids, which was previously observed in amorphous a–As$_x$S$_{1-x}$ system with a low As concentration [33, 45] and in g–Ge$_x$As$_{10}$S$_{90-x}$ with a low Ge content [46]. In addition, the band at 335 cm^{-1} is related to the symmetric stretching $As-S$ mode with the four-fold coordinated As atom in

the local quasi-tetrahedral structure of binary As$_x$S$_{1-x}$ glasses for $0.08 \leq x \leq 0.37$, as revealed from Raman scattering and supported by the first-principles cluster calculations [47]. Recently, Chrissanthopoulos *et al.* [48], using the first-principles cluster calculations or density functional theoretical (DFT) calculations performed for the GeS$_2$–In$_2$S$_3$–AgI glasses, have shown that the band at 335 cm^{-1} is also attributed to the symmetric stretching $Ge-S$ mode in the GeS$_4$ tetrahedra. In other words, due to similar electronic structure for As and Ge atoms, both the symmetric stretching $As-S$ mode in the quasi-tetrahedral units and the symmetric stretching $Ge-S$ mode in the tetrahedral units are nearly degenerate at 335 cm^{-1} from DFT calculations. However, since the symmetric stretching $As-S$ mode with the four-fold coordinated As atom was also observed experimentally by Raman measurements of the S-rich glasses of As$_x$S$_{1-x}$ system [47], we believe that the detected new band at 335 cm^{-1} instead of 342 cm^{-1} under radiation is correctly attributed to the symmetric stretch vibrations of $As-S$ bonds.

Why spectral changes are detected only in the VH configuration under radiation? To answer, we assume that the suggestion made for a-Se [18], explaining photo-

induced peaks in the VH configuration of Raman spectra, should be applied in our case accepting a similarity between light- and γ-induced effects in chalcogenide glasses [49, 50]. Thus, for instance, one of the reasons is that the radiation-induced peaks may be more clearly pronounced in the VH configuration, since the signal in the depolarized configuration is smaller than that in the polarized one.

Large depolarization ratios (Fig. 2) are associated with intrinsic anisotropy of the glasses, and the increase in depolarization ratio can be accompanied by the increase in the inelastic Raman scattering cross section [51]. The largest depolarization ratio is detected in the BP range, $\rho(\omega) \sim 0.6$, and consequently the intrinsic anisotropy of the glass can be explained by MRO features tightly related with the BP parameters. The small effect observed at the increase of the depolarization ratio in the BP range in the γ-irradiated state (insert, Fig. 2) testifies existence of possible radiation-induced additional intrinsic anisotropy in the glass studied on the MRO scale. The observed effect correlates with known photo-induced anisotropy in chalcogenide glasses [52]. Sharper drop in the depolarization ratio of the γ-irradiated sample as compared to unirradiated one in the high-frequency region of the depolarization ratio spectra can be caused by decreasing the inelastic Raman scattering cross section, probably, due to radiation-structural transformations. Appearance of a new local minimum within the range 300 to 400 cm^{-1} under radiation confirms atomic rearrangement in the glass backbone resulting in formation of radiation-induced defects.

The differential VH Raman spectra ($I^R_{\text{irrad.}} - I^R_{\text{unirrad.}}$) (Fig. 3) seem to be important similarly to conventional IR FFT spectra of additional γ-induced reflectivity [27]. Namely, the differential procedure allows to separate the chemical bonds formed within radiation-induced structural transformations (upper zero) with that preferred in the unirradiated state (under zero). The observed appearance of positive and negative intensity peaks only for the glass composition with $x = 0.4$, while the spectral changes are practically absent in the case of the glass compositions with $x = 0.1, 0.2$ and 0.6, shows clearly that the specific radiation-induced structural transformations occur exclusively for the alloy with $x = 0.4$. According to the XRD and EXAFS study of the stoichiometric arsenic-germanium sulfide glasses of $(As_2S_3)_x(GeS_2)_{1-x}$ system ($0.0 \le x \le 1.0$) [53] in combination with the reverse Monte-Carlo simulation [54], the structural order of As-rich ($x > 0.4$) and Ge-rich ($x < 0.4$) glasses is organized by the main $As-S$ and $Ge-S$ structural motifs based on pyramidal AsS_3 and tetrahedral GeS_4 units linked by $=As-S-As=$ and $\equiv Ge-S-Ge\equiv$ structural configurations, respectively, whereas for the intermediate compound with $x = 0.4$, the structural network is better homogeneous on the nanoscale due to appearance of $\equiv Ge-S-As=$ mixed structural configurations, and the structure of this alloy is similar to the structure of the stoichiometric glass $Ge_{18.2}As_{18.2}S_{63.6}$ (i.e., $x = 0.455$) consisting of a corner-shared network of homogeneously mixed GeS_4 tetrahedra and AsS_3 pyramids reported by Soyer-Uzun *et al.* [55]. The existence of $\equiv Ge-S-As=$ mixed structural configurations supports the γ-induced covalent bond switching heteropolar or heteronuclear $Ge-S$ bonds into heteropolar or heteronuclear $As-S$ ones [*the reaction* (*1*) with the $\equiv Ge-S-As=$ configuration: $(Ge-S)\rightarrow(As-S)$] accompanied by formation of atomic pairs of positively charged over-coordinated arsenic and negatively charged under-coordinated germanium ($As_4^+ + Ge_3^-$), the so-called coordination defects or valence alternation pairs (VAPs) [56], as shown schematically in Fig. 6 (the plus (+) sign indicates that there is no chemical bond between the charged centers [57]). This reaction (1) agrees well with appearance of the positive intensity peak in the vicinity of $325-335$ cm^{-1} (Fig. 3), corresponding to the vibrations of $As-S$ bonds, created under radiation, in the local structural configuraions with the four-fold coordinated As atom (i.e., As_4^+ defects).

Other two positive intensity peaks are observed in the vicinity of $420-430$ cm^{-1} and 490 cm^{-1} for the alloy with $x = 0.4$, while the splitting of the negative intensity band with the clear two peaks at 340-350 and $370-375$ cm^{-1} takes place (Fig. 3). As mentioned above, the positive intensity peaks at 430 and 490 cm^{-1} are related to the edge-sharing tetrahedra or $S-S$ dimers at the edge of "outrigger raft" clusters and covalent $S-S$ bonds, respectively. The negative two peaks at 340 and 370 cm^{-1} correspond to A_1 symmetric mode of $Ge-S$ bond vibrations in the corner-shared GeS_4 tetrahedra and A_1^c companion mode of $Ge-S$ bond vibrations in the edge-shared GeS_4 tetrahedra, respectively, although the structural origin of the companion mode remains a subject of considerable controversy [36, 58].
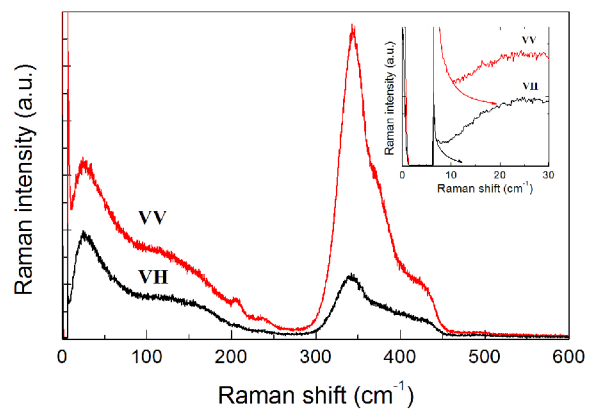

Fig. 4. The polarized-VV and depolarized-VH Raman spectra of $(As_2S_3)_{0.2}(GeS_2)_{0.8}$ glass, taken as an example, with the excess quasi-elastic light scattering in the low-frequency vibrational region well fitted using the Theodorakopoulos-Jäckle model [28] as shown schematically by lines with arrows in insert (see the text for details).
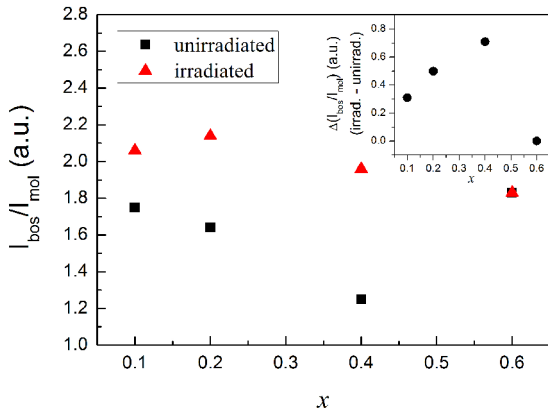
Fig. 5. The ratio of the intensity of the boson peak to the intensity of the main molecular peak at $340\ \text{cm}^{-1}$, I_{bos}/I_{mol}, for unirradiated and γ-irradiated glasses of the $(As_2S_3)_x(GeS_2)_{1-x}$ system as a function of composition x. Insert shows the difference, $\Delta(I_{bos}/I_{mol})$, between values of I_{bos}/I_{mol} for γ-irradiated (irrad.) and unirradiated (unirrad.) samples.
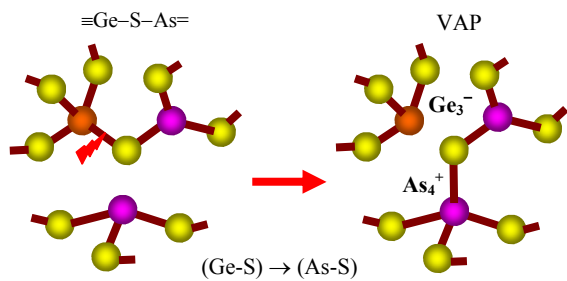

Fig. 6. The schematical illustration of γ-induced covalent bond switching heteropolar or heteronuclear Ge – S bonds into heteropolar or heteronuclear As – S bonds [*the reaction (1)* with the ≡ Ge – S – As = configuration: (Ge – S)→(As – S)] accompanied by formation of atomic pairs of positively charged over-coordinated arsenic and negatively charged under-coordinated germanium $As_4^+ + Ge_3^-$, VAP defects (see the text for details).
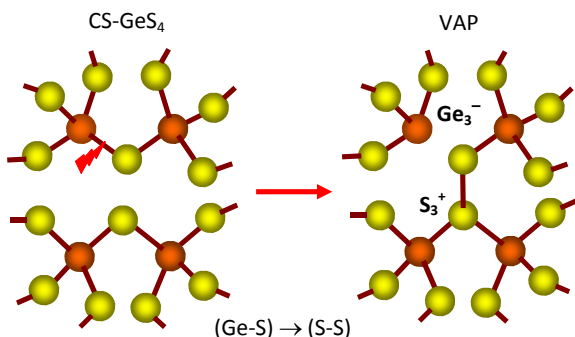

Fig. 7. The schematical illustration of γ-induced covalent bond switching heteropolar or heteronuclear Ge − S bonds in the corner-shared (CS) tetrahedral configuration into homopolar or homonuclear S − S bonds [*the reaction (2)* with the CS-GeS$_4$ configuration: (Ge – S)→(S – S)] accompanied by formation of atomic pairs of positively charged over-coordinated sulfur and negatively charged under-coordinated germanium ($S_3^+ + Ge_3^-$), VAP defects (see the text for details).

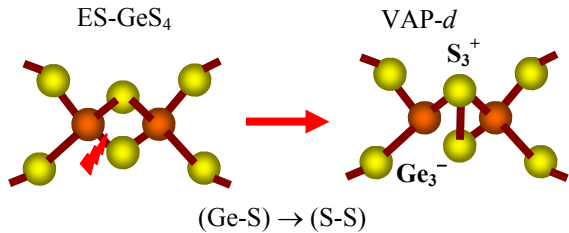**Fig. 8.** The schematical illustration of γ-induced covalent bond switching heteropolar or heteronuclear Ge − S bonds in the edge-shared (ES) tetrahedral configuration into homopolar or homonuclear S − S bonds [*the reaction (3)* with the ES-GeS$_4$ configuration: (Ge − S)→(S − S)] accompanied by formation of bound atomic pairs of positively charged over-coordinated sulfur and negatively charged under-coordinated germanium defects ($S_3^+ \cdot Ge_3^-$), VAP-*d* defects (see the text for details).

Appearance of the positive intensity peak at $490\ \text{cm}^{-1}$ (covalent S − S bonds) under radiation can be explained by the γ-induced covalent bond switching heteropolar or heteronuclear Ge − S bonds in the corner-shared (CS) tetrahedral configuration into homopolar or homonuclear S − S bonds [*the reaction (2)* with the CS-GeS$_4$ configuration: (Ge – S)→(S – S)] accompanied by formation of atomic pairs of positively charged over-coordinated sulfur and negatively charged under-coordinated germanium ($S_3^+ + Ge_3^-$), VAP defects (Fig. 7). These radiation-induced structural transformations (i.e., the reaction (2)) are suggested to be dominant in the case of Ge − Sb − S glasses of stoichiometric Sb$_2$S$_3$-GeS$_2$ system (examplified by Ge$_{23.5}$Sb$_{11.8}$S$_{64.7}$ glass) studied using high-resolution X-ray photoelectron spectroscopy (XPS) [59] as well as non-stoichiometric Sb$_2$S$_3$-Ge$_2$S$_3$ or Ge$_x$Sb$_{40-x}$S$_{60}$ system (examplified by Ge$_{25}$Sb$_{15}$S$_{60}$, Ge$_{27}$Sb$_{13}$S$_{60}$, and Ge$_{35}$Sb$_5$S$_{60}$ glasses) studied using high-energy synchrotron X-ray diffraction (XRD), extended X-ray absorption fine structure (EXAFS) spectroscopy and infrared spectroscopy [60–62].

Analyzing spectral changes in the vicinity of $430\ \text{cm}^{-1}$, special attention should be paid to understand better the origin of this mode with account of some experimental observations. Namely, the increase of the $430\ \text{cm}^{-1}$ mode with increasing the incident light energy found in g-GeS$_2$ indicates the existence of electronic states near the band edges leading to the reduction of S-based lone-pair (lp) states [58]. In interpretation of the $430\ \text{cm}^{-1}$ band assigned to the S − S dimers and/or edge-shared tetrahedra, both these units can be expected to contribute to formation of localized, band-tail states that, according to Yamaguchi *et al.* [58], are responsible for the resonance features of this mode in g-GeS$_2$. Comparatively, the relative intensities of the 430 and $490\ \text{cm}^{-1}$ S-related modes increase with growth in the incident light energy [58].

The similar interpretation is possible in the case of γ-irradiation-induced effect studied. The observed increase in the intensity of 490 cm^{-1} S-related mode (covalent $S-S$ bonds) under radiation according to the reaction (2), resulting in formation of the ($S_3^+ + Ge_3^-$) VAPs, agrees well with reduction of S-based lp states due to S_3^+ defects. It should be noted here that the reduction of S-based lp states caused by appearance of over-coordinated S atoms within the ($S_3^+ + Ge_3^-$) VAPs has also been supported by high-resolution XPS study of reversible γ-induced structural transformations in vitreous $Ge_{23.5}Sb_{11.8}S_{64.7}$ [59]. Alternatively, the observed increase in the intensity of 430 cm^{-1} S-related mode ($S-S$ dimers and/or edge-shared tetrahedra) under radiation seems to be related with reduction of S-based lp states owing to the γ-induced covalent bond switching heteropolar or heteronuclear $Ge-S$ bonds in the edge-shared (ES) tetrahedral configuration into homopolar or homonuclear $S-S$ bonds [*the reaction (3)* with the ES-GeS$_4$ configuration: $(Ge-S)\rightarrow(S-S)$] accompanied by formation of bound atomic pairs of positively charged over-coordinated sulfur and negatively charged under-coordinated germanium defects ($S_3^+ \cdot Ge_3^-$), known as valence alternation pairs dipole (VAP-*d*), as shown in Fig. 8 (the point ($\cdot$) sign indicates that there is a chemical bond between the charged centers [57]). Using the quantum-chemical modeling approach Dembovskii *et al.* [57] showed that the VAP-*d* defects are even more energetically favored than conventional VAP ones, but the VAP-*d* defects are more stable when the rigid environment around the defects does exist. Obviously, in the case of the reaction (3), this rigid environment around VAP-*d* ($S_3^+ \cdot Ge_3^-$) defects should be attained due to "outrigger raft" clusters in the ES-GeS$_4$ configuration [37]. The radiation-induced VAP-*d* ($S_3^+ \cdot Ge_3^-$) defects, schematically presented by the atomic-size model in Fig. 8, are also reported for the radiation-modified $Ge_{35}Sb_5S_{60}$ glass, as revealed from high-energy XRD measurements [60].

Boolchand *et al.* [36] noted that the density of vibrational states (DOVS) calculations in specific molecular clusters allows to interpret the companion A_1^c mode at 370 cm^{-1} as a cluster edge mode as well as the 430 cm^{-1} mode is also typical to the $S-S$ stretch coming from cluster edge dimers. So, on the one hand, the DOVS calculations indicate the 370 and 430 cm^{-1} modes seem to be interrelated. On the other hand, recent *ab-initio* or DFT calculations of Raman spectra in GeS$_2$ glass [63] showed the 370 cm^{-1} feature can be attributed to the companion A_1^c mode of vibrations in edge-shared tetrahedra. It means from the theoretical viewpoint that changes in the vibrational properties in the ES-GeS$_4$ (370 cm^{-1}) and $S-S$ cluster edge dimers (430 cm^{-1}) are supposed to be correlated. The obtained results agree well with the above mentioned theoretical calculations,

giving therefore the first experimental evidence of correlation between the 370 and 430 cm^{-1} modes as far as we know.

The composition dependence of the disorder degree examplified by the ratio of I_{bos}/I_{mol} (Fig. 5) supports the specific radiation-induced structural changes observed for the alloy with $x = 0.4$. Namely, in the unirradiated state, the minimum value of I_{bos}/I_{mol} attained at $x = 0.4$ ($Ge_{15.8}As_{21}S_{63.2}$) testifies the smallest degree of disorder for this compound, most probably, due to the existence of $\equiv Ge-S-As =$ mixed structural configurations resulting in the best homogeneous structure similarly to the structure of the stoichiometric glass $x = 0.455$ ($Ge_{18.2}As_{18.2}S_{63.6}$) consisting of a corner-shared network of homogeneously mixed GeS$_4$ tetrahedra and AsS$_3$ pyramids [55]. At the same time, the radiation-induced change in the I_{bos}/I_{mol} magnitude $\Delta(I_{bos}/I_{mol}) = ([I_{bos}/I_{mol}]_{irrad.} - [I_{bos}/I_{mol}]_{unirrad.})$ is found to be the largest for the alloy with $x = 0.4$ (insert, Fig. 5), showing the essential increase of the disorder degree under radiation. We believe that this funding is due to the best homogeneous structure of the glass leading to the favoured conditions for the above mentioned reactions (1)-(3) (Figs. 6-8) and, thus, to the radiation-induced structural changes on the short- and medium-range order scales.

5. Conclusions

Radiation-induced structural changes in the chalcogenide glasses of the $(As_2S_3)_x(GeS_2)_{1-x}$ system ($x = 0.1, 0.2, 0.4, 0.6$) have been studied in detail by using the Raman spectroscopy technique. Employing the differential representation of the depolarized (VH) Raman spectra measured for the γ-irradiated and unirradiated samples, it has been found that the radiation-induced structural changes are significant only for the glass composition with $x = 0.4$, while these changes are practically absent in the case of the glass compositions with $x = 0.1, 0.2$ and 0.6. The applied differential procedure has also allowed to detect the radiation-induced effects in clusters of corner-shared and edge-shared tetrahedra. It has been concluded that the controversial companion A_1^c mode at 370 cm^{-1} to the main 340 cm^{-1} A_1 symmetric mode of vibrations in corner-shared tetrahedra seems to be related mainly to the vibrations of edge-shared tetrahedra. The possible nanoscale structural mechanism to account for the observed spectral changes has been discussed. As a result, three γ-induced covalent bond switching reactions have been identified: *the reaction (1)* with the $\equiv Ge-S-As =$ configuration $[(Ge-S)\rightarrow(As-S)]$ accompanied by formation of ($As_4^+ + Ge_3^-$) VAP defects; *the reaction (2)* with the CS-GeS$_4$ configuration $[(Ge-S)\rightarrow(S-S)]$ accompanied by formation of ($S_3^+ + Ge_3^-$) VAP defects; and *the reaction (3)* with the ES-GeS$_4$ configuration $[(Ge-S)\rightarrow(S-S)]$ accompanied

by formation of ($S_3^+ \cdot Ge_3^-$) VAP-*d* defects. It has also been ascertained that the composition dependence of the disorder degree examplified by the ratio of I_{bos}/I_{mol} supports the specific radiation-induced structural changes detected for the alloy with $x = 0.4$.

Acknowledgments

References

1. 1. K. Shimakawa, A.V. Kolobov, S.R. Elliott, Photo-induced effects and metastability in amorphous semiconductors and insulators // *Adv. Phys.*, **44**(6), p. 475-588 (1995).
2. K. Tanaka, Photo-induced structural changes in amorphous semiconductors // *Semiconductors*, **32**(8), p. 861-866 (1998).
3. A.V. Stronski, Some peculiarities of the mechanism of irreversible photostructural transformations in thin As-S-Se layers // *Semiconductor Physics, Quantum Electronics & Optoelectronics*, **4**(2), p. 111-117 (2001).
4. A.V. Stronski, M. Vlcek, S.A. Kostyukevych, V.M. Tomchuk, E.V. Kostyukevych, S.V. Svechnikov, A.A. Kudryavtsev, N.L. Moskavenko, A.A. Koptyukh, Study of non-reversible photostructural transformations in $As_{40}S_{60-x}Se_x$ layers applied for fabrication of holographic protective elements // *Semiconductor Physics, Quantum Electronics & Optoelectronics*, **5**(3), p. 284-287 (2002).
5. A.V. Stronski, M. Vlček, Photosensitive properties of chalcogenide vitreous semiconductors in diffractive and holographic technologies applications // *J. Optoelectron. Adv. Mater.*, **4**(3), p. 699-704 (2002).
6. O.I. Shpotyuk, R.Ya. Golovchak, T.S. Kavetsky, A.P. Kovalskiy, M.M. Vakiv, Radiation-optical effects in glassy Ge-As(Sb)-S systems // *Nucl. Instrum. Methods Phys. Res. B*, **166-167**, p. 517-520 (2000).
7. O.I. Shpotyuk, Radiation-induced effects in chalcogenide vitreous semiconductors // *Semiconducting Chalcogenide Glass I: Glass Formation, Structure, and Stimulated Transformations in Chalcogenide Glasses, Semiconductors and Semimetals, ed. by R. Fairman and B. Ushkov.* Elsevier Academic Press, **78**, p. 215-260 (2004).
8. G.A.M. Amin, N.M. Spyrou, Study of gamma-irradiation-induced optical effects in Ge-Se-Cd for possible industrial dosimetric applications // *Radiation Physics and Chemistry*, **72**, p. 419-422 (2005).
9. T.S. Kavetskyy, Impact of the sample thickness and γ-irradiation dose on the occurrence of radiation-induced optical effects in chalcogenide vitreous semiconductors of the Ge-Sb-S system // *Semiconductors*, **45**(4), p. 499-502 (2011).
10. I.V. Chepeleva, K.K. Ermakovich, Yu.S. Tver'yanovich, Formation of radiation-induced defects in glasses of the copper-arsenic-selenium system // *Glass Physics and Chemistry*, **29**(2), p. 160-165 (2003).
11. V.O. Balitska, O.I. Shpotyuk, On the problem of electron-induced anisotropy effect in As_2S_3-based glasses // *Nucl. Instrum. Methods Phys. Res. B*, **166-167**, p. 521-524 (2000).
12. H.Z. Tao, G.P. Dong, H.Y. Xiao, C.G. Lin, X.J. Zhao, Second-order nonlinear optical properties of Ge-Ga-Ag-S glass irradiated by electron beam // *Trans. Nonferrous Met. Soc. China*, **16**, p. s170-s173 (2006).
13. M.M. Pop, M.O. Malets, I.I. Shpak, D.G. Semak, Electron-induced changes of optico-refractometric parameters of glassy alloys of the Sb_2S_3-GeS_2 system // *Ukr. J. Phys.*, **55**(8), p. 912-916 (2010).
14. S.K. Tripathi, A. Thakur, G. Singh, J. Sharma, V. Sharma, K.P. Singh, G.S.S. Saini, N. Goyal, Irradiation effects on the optical properties of a-Ge-Se-Ag thin films // *J. Optoelectron. Adv. Mater.*, **7**(4), p. 2095-2101 (2005).
15. M. Frumar, A.P. Firth, A.E. Owen, A model for photostructural changes in the amorphous As-S system // *J. Non-Cryst. Solids*, **59-60**, p. 921-924 (1983).
16. M. Frumar, Z. Polak, Z. Cernosek, Raman spectra and photostructural changes in the short-range order of amorphous As-S chalcogenides // *J. Non-Cryst. Solids*, **256-257**, p. 105-110 (1999).
17. M. Frumar, A.P. Firth, A.E. Owen, Optically induced crystal-to-amorphous-state transition in As_2S_3 // *J. Non-Cryst. Solids*, **192-193**, p. 447-450 (1995).
18. A. Kolobov, H. Oyanagi, A. Roy, K. Tanaka, Role of lone-pair electrons in reversible photostructural changes in amorphous chalcogenides // *J. Non-Cryst. Solids*, **227-230**, p. 710-714 (1998).

19. I.P. Kotsalas, D. Papadimitriou, C. Raptis, M. Vlcek, M. Frumar, Raman study of photo-structural changes in amorphous $Ge_xSb_{0.4-x}S_{0.6}$ // *J. Non-Cryst. Solids*, **226**, p. 85-91 (1998).

20. R. Ston, M. Vlcek, H. Jain, Structure and photo-induced changes in bulk and films of As-Ge-S system // *J. Non-Cryst. Solids*, **326-327**, p. 220-225 (2003).

21. R. Holomb, N. Mateleshko, V. Mitsa, P. Johansson, A. Matic, M. Veres, New evidence of light-induced structural changes detected in As-S glasses by photon energy dependent Raman spectroscopy // *J. Non-Cryst. Solids*, **352**, p. 1607-1611 (2006).

22. T. Kavetskyy, M. Vakiv, O. Shpotyuk, Charged defects in chalcogenide vitreous semiconductors studied with combined Raman scattering and PALS methods // *Radiation Measurements*, **42**, p. 712-714 (2007).

23. A. Feltz, *Amorphous and Vitreous Inorganic Solids.* Mir, Moscow, 1986 (in Russian).

24. O.I. Shpotyuk, A.P. Kovalskiy, T.S. Kavetskyy, R.Ya. Golovchak, Threshold restoration effects in γ-irradiated chalcogenide glasses // *J. Non-Cryst. Solids*, **351**, p. 993-997 (2005).

25. T.S. Kavetskyy, O. Šauša, V.F. Valeev, V.I. Nuzhdin, N.M. Lyadov, A.L. Stepanov, Raman, positron annihilation and Doppler broadening spectroscopy of gamma-irradiated and Cu-ion implanted $Ge_{15.8}As_{21}S_{63.2}$ glass // *In: Coherent Optics and Optical Spectroscopy*, ed. by M.Kh. Salakhov, Kazan Univ., p. 86-89 (2011).

26. T. Kavetskyy, S. Yannopoulos, Raman spectroscopy study of radiation-induced structural changes in chalcogenide glasses // *In: Abstracts of International Conference "Advanced Optical Materials and Devices" (AOMD-7)*, Vilnius, Lithuania, p. 22 (2011).

27. R.Ya. Golovchak, O.I. Shpotyuk, Radiation-induced bond switching in mixed Ge-As sulphide glasses // *Phil. Mag.*, **85**(25), p. 2847-2860 (2005).

28. N. Theodorakopoulos, J. Jäckle, Low-frequency Raman scattering by defects in glasses // *Phys. Rev. B*, **14**(6), p. 2637-2641 (1976).

29. D. Arsova, E. Skordeva, D. Nesheva, E. Vateva, A. Perakis, C. Raptis, A comparative Raman study of the local structure in $(Ge_2S_3)_x(As_2S_3)_{1-x}$ and $(GeS_2)_x(As_2S_3)_{1-x}$ glasses // *Glass Phys. Chem.*, **26**(3), p. 247-251 (2000).

30. Y.C. Boulmetis, A. Perakis, C. Raptis, D. Arsova, E. Vateva, D. Nesheva, E. Skordeva, Composition and temperature dependence of the low-frequency Raman scattering in Ge-As-S glasses // *J. Non-Cryst. Solids*, **347**, p. 187-196 (2004).

31. Y.C. Boulmetis, C. Raptis, D. Arsova, Structure and dynamics of Ge-As-S chalcogenide glasses monitored by low-frequency Raman scattering // *J. Optoelectron. Adv. Mater.*, **7**(3), p. 1206-1216 (2005).

32. G. Lucovsky, F.L. Galeener, R.C. Keezer, R.H. Geils, H.A. Six, Structural interpretation of infrared and Raman spectra of glasses in the alloy system $Ge_{1-x}S_x$ // *Phys. Rev. B*, **10**(12), p. 5134-5146 (1974).

33. T. Mori, K. Matsuishi, T. Arai, Vibrational properties and network topology of amorphous As-S systems // *J. Non-Cryst. Solids*, **65**, p. 269-283 (1984).

34. A.V. Stronski, M. Vlcek, I.D. Tolmachov, H. Pribylova, Optical characterization of As-Ge-S thin films // *J. Optoelectron. Adv. Mater.*, **11**(11), p. 1581-1585 (2009).

35. J. Sukmanowski, I. Petscherizin, M. Soltwisch, D. Quitmann, Raman scattering from a partly interrupted network glass former // *J. Phys.: Condens. Matter*, **2**, p. 2303-2330 (1990).

36. P. Boolchand, J. Grothaus, M. Tenhover, M.A. Hazle, R.K. Grasselli, Structure of GeS_2 glass: Spectroscopic evidence for broken chemical order // *Phys. Rev. B*, **33**(8), p. 5421-5434 (1986).

37. P.M. Bridenbaugh, G.P. Espinosa, J.E. Griffiths, J.C. Phillips, J.P. Remeika, Microscopic origin of the companion A_1 Raman line in glassy $Ge(S,Se)_2$ // *Phys. Rev. B*, **20**(10), p. 4140-4144 (1979).

38. R.J. Nemanich, G.A.N. Connell, T.M. Hayes, R.A. Street, Thermally induced effects in evaporated chalcogenide films. I. Structure // *Phys. Rev. B,* **18**(12), p. 6900-6914 (1978).

39. A.T. Ward, Raman spectroscopy of sulfur, sulfur-selenium, and sulfur-arsenic mixtures // *J. Phys. Chem.*, **72**(12), p. 4133-4139 (1968).

40. B.R. Johnson, M.J. Schweiger, S.K. Sundaram, Chalcogenide nanowires by evaporation-condensation // *J. Non-Cryst. Solids*, **351**, p. 1410-1416 (2005).

41. A.P. Paiuk, A.V. Stronski, M. Vlček, A.A. Gubanova, Ts.A. Krys'kov, P.F. Oleksenko, Peculiarities of As-S glass structure doped with ytterbium // *Proc. SPIE*, **8306**, 830617-1-830617-4 (2011).

42. A.P. Paiuk, I.M. Lishchynskyy, A.V. Stronski, M. Vlček, A.A. Gubanova, Ts.A. Krys'kov, P.F. Oleksenko, Changes of properties of As_2S_3 at doping by rare-earth and transition metals: DSC investigation and Raman spectroscopy // *Optoelektronika i poluprovodnikovaia tekhnika*, **46**, p. 62-67 (2011), in Ukrainian.

43. F. Kyriazis, A. Chrissanthopoulos, V. Dracopoulos, M. Krbal, T. Wagner, M. Frumar, S.N. Yannopoulos. Effect of silver doping on the structure and phase separation of sulfur-rich As-S glasses: Raman and SEM studies // *J. Non-Cryst. Solids*, **355**, p. 2010-2014 (2009).

44. R. Holomb, P. Johanson, V. Mitsa, I. Rosola, Local structure of technologically modified g-GeS2: resonant Raman and absorption edge spectroscopy combined with *ab initio* calculations // *Phil. Mag.* **85**(25), p. 2947-2960 (2005).

45. T. Wagner, S.O. Kasap, M. Vlcek, A. Sklenar, A. Stronski, The structure of As_xS_{100-x} glasses

studied by temperature-modulated differential scanning calorimetry and Raman spectroscopy // *J. Non-Cryst. Solids*, **227-230**, p. 752-756 (1998).

46. M. Pisarcik, L. Koudelka, Raman spectra and structure of Ge-As-S glasses in the S-rich region // *Materials Chemistry*, **7**, p. 499-508 (1982).

47. P. Chen, C. Holbrook, P. Boolchand, D.G. Georgiev, K.A. Jackson, M. Micoulaut, Intermediate phase, network demixing, boson and floppy modes, and compositional trends in glass transition temperatures of binary As_xS_{1-x} system // *Phys. Rev. B*, **78**(22), 224208-1-224208-15 (2008).

48. A. Chrissanthopoulos, P. Jóvári, I. Kaban, S. Gruner, T. Kavetskyy, J. Borc, W. Wang, J. Ren, G. Chen, S.N. Yannopoulos. Structure of AgI-doped Ge-In-S glasses: Experiment, reverse Monte Carlo modelling, and density functional calculations // *J. Solid State Chem.*, **192**, p. 7-15 (2012).

49. A. Kovalskiy, T. Kavetskyy, Ju. Plewa, O. Shpotyuk, Interpretation of radiation-induced phenomena in chalcogenide glasses of Ge-Sb-S system using free volume and covalent chemical bonds concepts // *Solid State Phenomena*, **90-91**, p. 241-246 (2003) (and references therein).

50. O.I. Shpotyuk, T.S. Kavetskyy, A.P. Kovalskiy, Phenomenological model of radiation-induced optical effects in Sb_2S_3-GeS_2(Ge_2S_3) chalcogenide glasses // *Proc. SPIE*, **5122**, p. 95-103 (2003) (and references therein).

51. V. Martinez, C. Martinet, B. Champagnon, R. Le Parc, Light scattering in SiO_2-GeO_2 glasses: quantitative comparison of Rayleigh, Brillouin and Raman effects // *J. Non-Cryst. Solids*, **345-346**, p. 315-318 (2004).

52. V. Lyubin, A.V. Kolobov, T. Yasuda, M. Klebanov, L. Boehm, K. Tanaka, Photo-induced reflectance anisotropy in chalcogenide glassy semiconductors // *J. Non-Cryst. Solids*, **227-230**, p. 677-681 (1998).

53. I. Kaban, T. Kavetskyy, P. Jovari, W. Hoyer, M.V. Zimmermann, M.A. Webb, XRD and EXAFS study of stoichiometric arsenic-germanium sulphide glasses // *HASYLAB Annual Report*, *http://hasylab.desy.de/annual_report/files/2009/20 09586.pdf* (2009).

54. T. Kavetskyy, S.N. Yannopoulos, P. Jóvári, I. Kaban, Part I. Structural order in $(As_2S_3)_x(GeS_2)_{1-x}$ ($0 \leq x \leq 1$) glasses // *to be published*.

55. S. Soyer-Uzun, C.J. Benmore, J.E. Siewenie, S. Sen, The nature of intermediate-range order in Ge-As-S glasses: results from reverse Monte Carlo modeling // *J. Phys.: Condens. Matter*, **22**, p. 115404 (2010).

56. M. Kastner, D. Adler, H. Fritzsche, Valence-alternation model for localized gap states in lone-pair semiconductors // *Phys. Rev. Lett.*, **37**, p. 1504-1507 (1976).

57. S.A. Dembovskii, A.S. Zyubin, F.V. Grigor'ev, Modeling of hypervalent configurations, valence alternation pairs, deformed structure, and properties of a-S and a-As_2S_3 // *Semiconductors*, **32**(8), p. 843-849 (1998).

58. M. Yamaguchi, T. Shibata, K. Tanaka, A resonance Raman scattering study of localized states in Ge-S glasses // *J. Non-Cryst. Solids*, **232-234**, p. 715-720 (1998).

59. A. Kovalskiy, H. Jain, A.C. Miller, R.Ya. Golovchak, O.I. Shpotyuk, A study of reversible γ-induced structural transformations in vitreous $Ge_{23.5}Sb_{11.8}S_{64.7}$ by high-resolution X-ray photoelectron spectroscopy // *J. Phys. Chem. B*, **110**, p. 22930-22934 (2006).

60. T. Kavetskyy, O. Shpotyuk, I. Kaban, W. Hoyer, Radiation-modified structure of $Ge_{25}Sb_{15}S_{60}$ and $Ge_{35}Sb_5S_{60}$ glasses // *J. Chem. Phys.*, **128**(24), 244514-1-244514-8 (2008).

61. T. Kavetskyy, O. Shpotyuk, V. Balitska, G. Dovbeshko, I. Blonskyy, I. Kaban, W. Hoyer, M. Iovu, A. Andriesh, Vibrational and structural properties of unmodified and radiation-modified chalcogenide glasses for advanced optical applications // *Proc. SPIE*, **7142**, 71420B-1-71420B-8 (2008).

62. T. Kavetskyy, I. Kaban, O. Shpotyuk, W. Hoyer, V. Tsmots, On the structural-optical correlations in radiation-modified chalcogenide glasses // *J. Phys.: Conf. Ser.*, **289**, 012007-1-012007-6 (2011).

63. N. Mateleshko, V. Mitsa, R. Holomb, Structural studies of technologically modified GeS_2 glasses and film // *Physica B: Condens. Matter*, **349**, p. 30-34 (2004).